High-pressure/high-temperature synthesis of transition metal oxide perovskites

High-pressure / High-temperature Synthesis of Transition Metal Oxide Perovskites

Jennifer A. Rodgers, Anthony J. Williams, and J. Paul Attfield

Centre for Science at Extreme Conditions and School of Chemistry, University of Edinburgh, King's Buildings, Mayfield Road, Edinburgh, EH9 3JZ, United Kingdom

Reprint requests to J. P. Attfield. E-mail: j.p.attfield@ed.ac.uk

Z. Naturforsch. **61b,** 1515 – 1526 (2006); received July 13, 2006

Perovskite and related Ruddlesden-Popper type transition metal oxides synthesised at high pressures and temperatures during the last decade are reviewed. More than 60 such new materials have been reported since 1995. Important developments have included perovskites with complex cation orderings on A and B sites, multiferroic bismuth-based perovskites, and new manganites showing colossal magnetoresistance (CMR) and charge ordering properties.

Key words: High-pressure Synthesis, Perovskites, Cation Ordering

Introduction

The ABO_3 perovskite structure is common among ternary transition metal oxides, with many derived compositions and structures based on chemical substitutions at the A or B sites, or variations in the oxygen content [1]. These perovskites are particularly important because of a wide range of notable chemical and physical properties [2] such as ferroelectricity [3], ionic conductivity [4], catalysis [5], colossal magnetoresistances (CMR) in doped manganese perovskites [6], and superconductivity in layered copper oxides [7].

The ideal ABO_3 perovskite oxide structure (Fig. 1a) is cubic, with $Pm3m$ space group symmetry and a typical lattice parameter $a_p \sim 4$ Å. The A and B cations have regular 6- (octahedral) and 12-fold coordinations. However, ordered tilts and rotations of the BO_6 octahedra frequently result in lower symmetry superstructures which have been analysed using group theory [8, 9]. Further superstructures are generated by ordering of cations; one of the most common is the elpasolite (K_2NaAlF_6) or 'double perovskite' structure (Fig. 1b) in which the B-site cations are ordered in a rocksalt-type substructure.

Several structural families are derived from the perovskite structure, a notable example is the Ruddlesden-Popper series $(AO)_{n+1}(BO_2)_n$ obtained by inserting an extra AO layer for every n BO_2 layer in the perovskite arrangement. For $n = 1$, this generates the K_2NiF_4-type

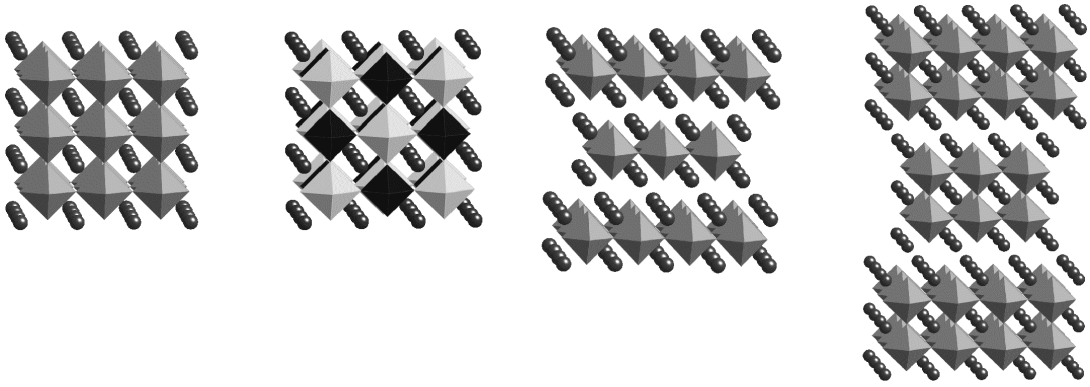

a b c d

Fig. 1. Polyhedral representations of (a) the ideal cubic perovskite, (b) the cation ordered (elpasolite) double perovskite structure, and (c) $n = 1$ (A_2BO_4) and (d) $n = 2$ ($A_3B_2O_7$) members of the Ruddlesden-Popper family of compounds.

Table 1. Composition, reported synthesis pressures and temperatures, structure type, space group and references for materials containing scandium B-site cations.

Composition	Pressure (GPa)	Temperature (°C)	Structure type	Space group	Ref.
$BiScO_3$	6	1140	Pv	*C*2/*c*	[10]
$BiScO_3 - PbTiO_3$	6	700 – 1250	Pv, ss	–	[11]

Table 2. Composition, reported synthesis pressures and temperatures, structure type, space group and references for materials containing titanium group B-site cations.

Composition	Pressure (GPa)	Temperature (°C)	Structure type	Space group	Ref.
$La_{1-x}K_xTiO_3$	4	980	Pv, ss	$Pm\bar{3}m$	[21]
$Eu_{0.62}K_{0.38}TiO_3$	4	900	Pv, ss	$Pm\bar{3}m$	[22]
$K_{2/3}Th_{1/3}TiO_3$	6	1200	Pv, pA	*P*4/*mmm*	[23]
$NdAgTi_2O_6$	14 – 14.5	1000	Pv, pA	*P*4/*nbm*	[24]
$Ca_2NdAgTi_4O_{12}$	14 – 14.5	1000	Pv, ss	$Pnm\bar{a}$	[24]
Ca_2TiSiO_6	14	1200	Pv, B	$Fm\bar{3}m$	[25]
$CaFeTi_2O_6$	14 – 14.5	1000	Pv, A	$P4_2/nm\ c$	[26]
$Bi_{0.5}Ag_{0.5}TiO_3$	12 – 15	1200 – 1400	Pv, ss	*Ibam*	[27]

structure (Fig. 1c) containing single layers of BO_6 octahedra in which two-dimensional physical properties are found, *e.g.* superconductivity in doped La_2CuO_4.

The stability of perovskites is determined to a first approximation by the ratio of A–O to B–O bond lengths, expressed as the tolerance factor, $t = (r_A + r_O)/\sqrt{2}(r_B + r_O)$ where r_i are the ionic radii. Materials with $0.85 < t < 1$ are usually stable. The different compressibilities of A–O and B–O bonds enable perovskites with lower (ambient pressure) tolerance factors to be stabilised at high pressure and quenched to ambient conditions. High-pressure reactions in the presence of an oxidant (*e. g.* $KClO_3$) may be used to stabilise high transition metal oxidation states, and high pressures also increase the rates of the high-temperature solid state reactions in which perovskites are formed by ionic diffusion between component oxides. High-pressure (1 – 10 GPa) high-temperature (∼ 1000 °C) (HPHT) reactions have been used to prepare perovskites since *ca.* 1970. In this review we survey new transition metal oxide perovskites prepared by HPHT synthesis during the last decade.

Review of New HPHT Transition Metal Oxide Perovskites

New HPHT perovskite oxides reported since 1995 are shown in Tables 1 – 9. Several materials that were reinvestigated following much earlier reports are also included. The phases have been classified according to the earliest transition metal group of the B-site cation(s). For each material, the composition (with A cations shown first), reported synthesis pressure and temperature, the structure type (Pv: perovskite, ss: solid solution, A: A-site order, pA: partial A site order, B: B-site order, RP1: n = 1 Ruddlesden-Popper, RP2: n = 2 Ruddlesden-Popper) and the space group are given.

Scandium

The perovskite $BiScO_3$ [10] has been synthesised under high-pressure / high-temperature conditions, and is of interest due to the potential of the highly polarisable Bi^{3+} cation to yield technologically important ferroic properties, such as those observed in the magnetic analogues $BiFeO_3$ [12 – 14] and $BiMnO_3$ [15–20]. $BiScO_3$, however, is reported to be centrosymmetric, crystallising in the monoclinic space group *C*2/*c*. The Bi–O bond lengths, obtained from Rietveld refinement, suggest that the Bi^{3+} lone pair is active in $BiScO_3$, and that neighbouring Bi atoms exhibit an antiparallel displacement along the *b* direction.

The solid solutions $x BiScO_3 - (1–x)PbTiO_3$ [11] have also been prepared by HPHT techniques. Changes in the crystal symmetry are observed with increasing *x*, from tetragonal to rhombohedral to *pseudo* cubic, to monoclinic to triclinic. Dielectric measurements suggest ferroelectric behaviour in the tetragonal, rhombohedral and *pseudo* cubic phases, but not for the monoclinic one.

Titanium group

High-pressure / high-temperature synthesis is used to prepare many mixed valence perovskite oxides, including those containing a mixture of Ti^{3+}/Ti^{4+} ions. The perovskite solid solution $La_{1-x}K_xTiO_3$ [21] has recently been prepared, and has been shown by XPS and EPR measurements to contain mixed valence Ti, as well as A-cation vacancies, which both vary with the level of potassium doping, *x*. Similarly, the mixed valent titanate $Eu_{0.62}K_{0.38}TiO_3$ has been prepared [22],

Composition	Pressure (GPa)	Temperature (°C)	Structure type	Space group	Ref.
$PbVO_3$	4 – 6	700 – 750	Pv	*P*4*mm*	[31]
$Cd_{1-x}Na_xVO_3$	6	1000	Pv, ss	*Pnma*	[32]
$PbM_{1/2}Nb_{1/2}O_3$ (M = Y, Ho)	4 – 6	1400 – 1500	Pv, B	–	[33]
$RbLaSrNb_2MO_9$ (M = Cu, Mg, Zn)	5	1050	Pv, ss	–	[34]
$CaCu_3Ga_2Nb_2O_{12}$	12 – 12.5	1100	Pv, A	$Im\bar{3}$	[35]
$CaCu_3Ga_2Ta_2O_{12}$	12 – 12.5	1100	Pv, AB	$Pm\bar{3}$	[35]

Table 3. Composition, reported synthesis pressures and temperatures, structure type, space group and references for materials containing vanadium group B-site cations.

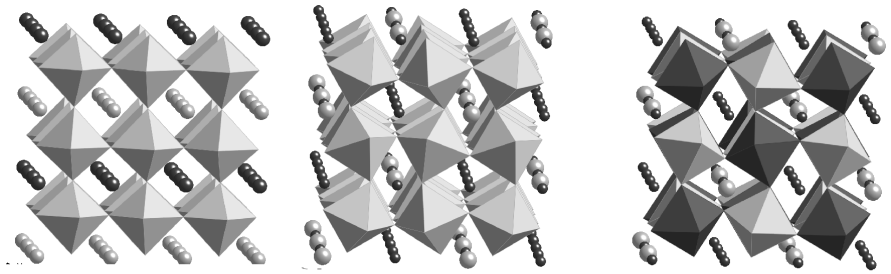

a b c

Fig. 2. A-site ordering within mixed cation perovskites; (a) $CaCu_3Ga_2Nb_2O_{12}$, (b) $NdAgTi_2O_6$, and (c) $CaCu_3Ga_2Ta_2O_{12}$ in which the B-site cations are also ordered.

although in this instance it is the europium ions that exhibit a mixed Eu^{2+}/Eu^{3+} valence. These perovskite systems are cubic, and are likely to be the subject of further study as their transport and magnetic properties are of potential interest.

Other HPHT syntheses of titanate perovskites have concentrated on the synthesis of Ti^{4+} double perovskites and solid solutions with novel structural arrangements. $K_{2/3}Th_{1/3}TiO_3$ [23] contains K^+ and Th^{4+} at the A site, which partially order along the [001] axis to yield a tetragonal *P*4/*mmm* structure. A similar layered ordering was observed in $NdAgTi_2O_6$ (Fig. 2b) containing monovalent silver [24], although in this instance an additional octahedral tilting lowers the symmetry to *P*4/*nbm*.

These two structures represent the first examples of perovskites synthesised under high pressures that contain such a layered ordering of A-site cations – an arrangement which has yielded many interesting physical properties when observed in ambient pressure transition metal oxide systems [28 – 30]. The perovskite $Ca_2NdAgTi_4O_{12}$ has also been prepared using HPHT techniques [24], although it contains a random distribution of $Ca^{2+}/Nd^{3+}/Ag^+$ ions at the A site.

Ca_2TiSiO_6 [25] is reported to be the first example of a double perovskite containing silicon as one of the B-site cations. X-ray diffraction studies show the B-site cations to be completely ordered in a rocksalt arrangement, giving a cubic $Fm\bar{3}m$ cell, with cell parameter $2a_P$.

A novel structural arrangement has been observed in HPHT-synthesised $CaFeTi_2O_6$ [26], which contains both calcium and iron on the perovskite A sites. These order into columns parallel to the *c*-axis, with a single Ca^{2+} site and two Fe^{2+} sites which alternate along the Fe column. Two independent tilts of the TiO_6 octahedra occur, reducing the symmetry of this system to $P4_2/nmc$, and yielding highly distorted A-cation environments – the effective coordination of the two iron sites becomes tetrahedral and square planar, respectively, the latter representing a very unusual geometry for Fe^{2+} ions.

The bismuth-containing perovskite $(Bi_{1/2}Ag_{1/2})TiO_3$ [27] has also been prepared under HPHT conditions. No A-site cation ordering was observed in this material, which exhibits an orthorhombic distortion to space group *Ibam* at r. t.. High-temperature phase transitions are observed to tetragonal *I*4/*mcm*, and then to cubic $Pm\bar{3}m$ symmetry above 673 K.

Vanadium group

The $3d^1$ perovskites, $A^{2+}V^{4+}O_3$, have been widely studied due to their diverse electronic properties [36 – 38]. A new perovskite $PbVO_3$ has recently been prepared [31] using high-pressure and high-temperature conditions. Due to the influence of the lone pair of the Pb^{2+} cation, the structure displays a strong tetragonal distortion (c/a = 1.23, space group *P*4*mm*), and

Composition	Pressure (GPa)	Temperature (°C)	Structure type	Space group	Ref.
$BiCrO_3$	4	720	Pv	*C*2, *Pnma*	[42]
$SrCr_{1-x}Ru_xO_3$ ($x = 0.4-0.6$)	3.5	1000	Pv, ss	*R*3*c*, *Pm*3*m*	[43]
$SrCr_{1-x}Ru_xO_3$ ($x = 0.8-1$)	10.5	1100	Pv, ss	*Pm*3*m*	
$CaCu_3Cr_2Sb_2O_{12}$	10	1100	Pv, AB	Pn3	[44]
$La_4Cu_3MoO_{12}$	6	1200	Pv, B	$P2_1/m$	[45]
$Ln_4Cu_3MoO_{12}$ (*Ln* = Pr, Nd, Sm)	6	1200	Pv, B	*P*1	[46]

Table 4. Composition, reported synthesis pressures and temperatures, structure type, space group and references for materials containing chromium group B-site cations.

the coordination of the vanadium atoms is best described as layers of corner-sharing square pyramids, rather than the normal octahedral perovskite framework. Resistivity measurements evidence semi conducting behaviour in $PbVO_3$ down to 2 K. Similarly, the vanadates $CdVO_3$ and $Cd_{0.8}Na_{0.2}VO_3$ have been prepared by HPHT [32], and were shown to have the $GdFeO_3$-type *Pnma* perovskite structure. They display metallic resistivities and Pauli paramagnetism between 1.8 and 300 K, analogous to the alkaline earth vandates $CaVO_3$ and $SrVO_3$.

Lead niobate materials, of general composition $PbRE_{1/2}{}^{3+}Nb_{1/2}O_3$, have been of interest owing to a variety of peculiarities in their crystal structure and physical properties [39–41], and the compounds with *RE* = Y and Ho have recently been prepared under HPHT conditions [33]. They revert to a cubic pyrochlore structure upon heating above 1000 K. The structure of the two materials is *pseudo* monoclinic ($\beta > 90°$, with $a = c$), and they are thought to be antiferroelectric, similar to other perovskites of the series (RE^{3+} = Lu–Dy). Another series of complex niobate perovskites, $RbLaSrNb_2MO_9$ (M = Cu, Mg, Zn) [34], have also been prepared by high-pressure treatment of hexagonal layered structures, although no cation ordering is apparent.

By contrast, the new perovskites $CaCu_3Ga_2Ta_2O_{12}$ and $CaCu_3Ga_2Nb_2O_{12}$ [35] display a complete cation ordering of Ca^{2+} and Cu^{2+} on the A sites (Fig. 2a, c). In addition, the tantalum compound exhibits a partial, rocksalt type Ga^{3+}/Ta^{5+} ordering on the B sites (the antimony analogue $CaCu_3Ga_2Sb_2O_{12}$, also prepared under high pressures, is fully ordered), and is thought to be the first example of A- and B-site ordering in a $AA'_3B_2B'_2O_{12}$-type perovskite. The structures of $CaCu_3Ga_2Ta_2O_{12}$ and $CaCu_3Ga_2Nb_2O_{12}$ were refined in cubic space groups *Pn*3̄ and *Im*3̄, respectively.

Chromium group

$BiCrO_3$, originally synthesised under HPHT conditions in 1968 [15], has recently been reinvestigated [42] with regard to possible multiferroic properties. At r. t., $BiCrO_3$ crystallises in monoclinic space group *C*2, as does the ferroelectric analogue $BiMnO_3$, before undergoing a structural phase transition to the centrosymmetric orthorhombic *Pnma* phase at 440 K. This transition is accompanied by an anomaly in the dielectric permittivity, identifying a ferroelectric transition. A parisitic ferromagnetic ordering occurs at 114 K.

The solid solution between $SrCrO_3$ and $SrRuO_3$ has been synthesised over the full range using a number of HPHT techniques [43]. The structure changes from orthorhombic *Pbnm* at low x through to rhombohedral *R*3̄*c* at $x = 0.4$, to cubic *Pm*3̄*m* for $0.5 < x < 1$, with no Cr/Ru order being observed at any doping level. Samples in the low Cr-doped regime are itinerant, and ferromagnetic, with the Curie temperature increasing with doping from 160 K up to a maximum T_C = 188 K. This, along with a substantial volume discontinuity near $x = 0.5$, evidences a substantial $Ru^{4+} + Cr^{4+} \rightarrow Ru^{5+} + Cr^{3+}$ charge transfer. An insulating regime is observed for $0.3 < x < 0.7$, and a G-type antiferromagnetic ordering with a high Néel temperature ($T_N \approx 400$ K) is observed for the rhombohedral $x = 0.4$ phase. The $0.7 < x < 1$ samples are itinerant and Pauli paramagnetic.

$CaCu_3Cr_2Sb_2O_{12}$ [44] has been synthesised at high-temperatures and pressures, and has an analogous structure to the Ga/Ta system described earlier – crystallising in cubic space group *Pn*3̄, and showing simultaneous cation ordering on both A and B sites. $CaCu_3Cr_2Sb_2O_{12}$ is insulating at all temperatures, but displays an abrupt increase in magnetisation below $\sim$ 160 K, which is attributed to soft ferrimagnetic behaviour.

The phases $RE_4Cu_3MoO_{12}$ (*RE* = La, Pr, Nd and Sm) all crystallise in the rare-earth $YMnO_3$-type hexagonal structure at ambient pressure. Recent studies [45, 46] have shown that they can be transformed at high pressure to a perovskite phase, which remains metastable at ambient pressure – not transforming back to the hexagonal form below 1073 K. These perovskites adopt a layered structure, with alternating layers of CuO_6 and $(Cu/Mo)O_6$ octahedra. Mag-

Composition	Pressure (GPa)	Temperature (°C)	Structure type	Space group	Ref.
$La_{1-x}Pb_xMnO_3$	5	1250 – 1300	Pv, ss	$-\underline{-}$	[47]
$RCu_3Mn_4O_{12}$ (R = Ln)	2	1000	Pv, A	$Im\bar{3}$	[48, 49]
$(Na_{0.25}Mn_{0.75})MnO_3$	–	–	Pv, B	*Im*3, *I*2/*m*	[50]
$BiMnO_3$	6	750	Pv	*C*2	[16]
Bi_2NiMnO_6	6	800	Pv, B	$C\underline{2}$	[51]
$Sr_8CaRe_3Cu_4O_{24}$	6	1300 – 1350	Pv, B	*Pm*3*m*	[52]

Table 5. Composition, reported synthesis pressures and temperatures, structure type, space group and references for materials containing manganese group B-site cations.

netisation measurements evidence two magnetic transitions – T_{N1} = 280 K in $La_4Cu_3MoO_{12}$, which decreases linearly in the other compounds with A-cation size, and T_{N2} = 25 K. The former is attributed to a two-dimensional antiferromagnetic ordering within the copper planes, whilst the latter is attributed to a weaker ordering within the mixed layers. Strontium can be substituted for lanthanum in $La_4Cu_3MoO_{12}$ up to 25%, changing the structure drastically from a layered monoclinic perovskite to an isotropic cubic perovskite. The resistivity of the sample also drops considerably on cooling; however it does not become metallic or superconducting.

Manganese group

The observation of colossal magnetoresistances (CMR) in manganese oxide perovskites has given rise to much research to understand and improve their properties [2, 6]. A wide variety of electronic and magnetic states has been observed in these compounds, and can be tuned by variations in chemical composition. The vast majority of manganites can be synthesised under ambient pressures, however in some specific cases, where small cations are situated on the perovskite A site yielding highly distorted structures, for example $YMnO_3$ [53], high-pressure synthesis conditions are essential. Stoichiometric $La_{1-x}Pb_xMnO_3$ (x = 0.6) solid solutions have been prepared under high-pressure conditions [47]. All samples have a slightly rhombohedrally distorted unit cell, and are ferromagnetic in the range $0.2 \leq x \leq 0.6$ with Curie temperatures up to 350 K. The sample with x = 0.4 exhibits metallic behaviour below T_m = 250 K, but samples with higher levels of Pb^{2+} doping are reported to be semiconducting.

The complex perovskite $CaCu_3Mn_4O_{12}$ has been of interest for some years, as it exhibits a considerable low field magnetoresistance at r. t., which is not coupled to the Curie temperature, T_C = 355 K. More recently, a series of analogous manganites have been prepared in which the Ca^{2+} cations are replaced by the trivalent rare earths La [49], Pr, Sm, Eu, Gd, Dy, Ho, Tm and Yb [48], with HPHT conditions being necessary for the synthesis in order to stabilise the small Cu^{2+} cations in the A position. In every case, the A cations are 3 : 1 ordered in a $2a_p \times 2a_p \times 2a_p$ cell of $Im\bar{3}$ symmetry. The r. t. magnetic structure of all the $RECu_3Mn_4O_{12}$ compounds involves a ferrimagnetic coupling between Mn^{3+}/Mn^{4+} and Cu^{2+} spins, and T_c increases with respect to the Ca analogue up to a value of approximately 400 K. $LaCu_3Mn_4O_{12}$ is shown to be metallic, in contrast to the Ca analogue, consistent with the carrier injection that results from replacement of Ca^{2+} by La^{3+}, and this effect also gives rise to an enhanced low field magnetoresistance.

The mixed valent manganite $(NaMn^{3+})(Mn^{3+}{}_2Mn^{4+}{}_2)O_{12}$, first synthesised under HPHT conditions in 1973 [54], has been reinvestigated recently [50] in order to understand the structural and magnetic properties of this complex perovskite. At r. t., it has a cubic structure, space group *Im*3, with only one B-site manganese position. There is a region of phase coexistence between 176 and 168 K, and below 168 K it adopts a monoclinic *I*2/*m* superstructure with an almost complete ordering of Mn^{3+} and Mn^{4+} charge states at the B sites, and an orbital ordering of the Mn^{3+} cations. At 125 K, the B site manganese moments order in a CE-type structure, whilst at around 92 K, the A site Mn moments order antiferromagnetically with an *anti* body-centred arrangement of spins. Resistivity measurements show a sudden increase in resistivity as temperature decreases through the charge ordering transition.

$BiMnO_3$, which requires high pressure for bulk synthesis, was first made in 1968 [15] and was shown to be ferromagnetic below 103 K. It has been the subject of more intense study in the last few years since theoretical predictions suggested it should be a multiferroic material [17]. Permittivity measurements have confirmed ferroelectricity [18] that persists below the ferromagnetic transition. $BiMnO_3$ adopts a highly distorted monoclinic structure [16], space group *C*2, with a transition to the centrosymmetric *Pnma* orthorhombic structure at $\sim$ 770 K. Recent measurements have also demonstrated a magnetocapaci-

Composition	Pressure (GPa)	Temperature (°C)	Structure type	Space group	Ref.
$Ca_{1-x}Sr_xFeO_3$	2	750 – 900	Pv	*Pnma*, *Pm*$\bar{3}$*m*	[55]
$CaFe_{1-x}Co_xO_3$	6	600 – 650	Pv	*Pnma*	[56]
$Sr_{2/3}La_{1/3}Fe_{1-x}Co_xO_3$	6	600 – 650	Pv	rhombohedral	
Pb_2FeMoO_6	4	800	Pv, B	–	[57]
$SrRu_{1-x}Rh_xO_3$	6	1500 – 1600	Pv	*Pnma*	[58]
$CaCu_3Ga_2Ru_2O_{12}$	12.5	1200	Pv, A	*Im*$\bar{3}$	[59]
$Sr_{3-x}Ba_xCaRu_2O_9$	8	1400	Pv, B	*P*$\bar{3}$*m*	[60]

Table 6. Composition, reported synthesis pressures and temperatures, structure type, space group and references for materials containing iron group B-site cations.

tance effect in the vicinity of the magnetic ordering temperature [20].

The new ferroelectric and ferromagnetic compound Bi_2NiMnO_6 has been prepared by high-pressure synthesis [51]. The crystal structure is a heavily distorted double perovskite, space group *C*2, with Ni^{2+} and Mn^{4+} ions ordered in a rocksalt coordination on the B site. The presence of the Bi^{3+} lone pair gives rise to ferroelectric properties with T_{CE} = 485 K, whilst magnetic measurements evidence a ferromagnetic transition at 140 K.

The novel perovskite phase $Sr_8CaRe_3Cu_4O_{24}$ has been prepared under HPHT conditions [52]. This phase has a cubic *Pm*$\bar{3}$*m* structure with a doubled periodicity along all three axes and complete ordering of the B-site Ca/Re/Cu cations onto crystallographically distinct sites, although the Re/Cu oxidation states are not known. The sample was shown to be ferromagnetic, with a transition temperature of around 440 K, and a spontaneous magnetisation of $\sim 1\mu_B$/f. u. Resistivity measurements showed insulating behaviour.

Iron group

The solid solution $Ca_{1-x}Sr_xFeO_3$ has been synthesised under HPHT conditions [55]. With increasing Sr content, the structure type is shown to change from orthorhombic, space group *Pnma*, to cubic, *Pm*$\bar{3}$*m*, with a possible phase coexistence being observed at $x \sim 0.6$. Within the orthorhombic regime, a metal-semiconductor transition is observed in the resistivity data, with the transition temperature dropping from 290 K for x = 0.0 to 200 K for x = 0.4. Neutron diffraction measurements on $Ca_{0.8}Sr_{0.2}FeO_3$ show this electronic transition to be coincident with a change in structural symmetry from orthorhombic to monoclinic $P2_1/m$. Comparison of the Fe–O bond lengths, and results from Mössbauer studies suggest that this is due to a charge disproportionation, $2Fe^{4+} \rightarrow Fe^{(4-\delta)+} + Fe^{(4+\delta)+}$, as previously observed for the end member $CaFeO_3$ [61], with δ increasing towards unity with decreasing temperature. Co-substitution studies of $CaFeO_3$ have also recently been conducted under high pressure, with $CaFe_{1-x}Co_xO_3$ crystallising in the $GdFeO_3$-type orthorhombic structure up to a solubility limit of x = 0.5 [56]. With increasing Co content, the insulating, antiferromagnetic, charge-disproportionated $CaFeO_3$ is seen to switch to a ferromagnetic, metallic phase with average Fe valences. A similar effect is observed for the $Sr_{2/3}La_{1/3}Fe_{1-x}Co_xO_3$ perovskite system [56].

A new Pb-analogue of the metallic ferromagnet Sr_2FeMoO_6 has recently been synthesised under high pressures [57]. X-ray diffraction measurements suggest that Pb_2FeMoO_6 has a partial ordering of B-site cations, while resistivity measurements show it to be semiconducting without appreciable magnetoresistance. A magnetic ordering is observed, but it is much weaker than in the strontium analogue, disappearing at T_N = 280 K.

In recent years, there has been considerable research interest in the ruthenate perovskites, due to the observation of a variety of interesting physical properties, including superconductivity in Sr_2RuO_4 [62]. The simple strontium ruthenate perovskite, $SrRuO_3$, which has an orthorhombic *Pbnm* perovskite structure has been of particular interest as it represents a rare example of a ferromagnetic 4*d*-transition metal oxide [63]. The solid solution $SrRu_{1-x}Rh_xO_3$ has been prepared using high-pressure techniques, substituting $4d^5$ Rh^{4+} for the $4d^4$ Ru^{4+}. As expected, considering the small difference in cation size, orthorhombic symmetry is maintained across the whole solid solution series. The ferromagnetic order is gradually suppressed with increasing rhodium doping, disappearing at $x \sim 0.6$, while resistivity measurements evidence metallicity for both end members, but semiconductor behaviour for the intermediate dopings, reaching a maximum at x = 0.6.

Double perovskite systems containing Ru^{5+} have been of interest due to the observation of unusual magnetic and transport properties [64 – 69], and in some cases, high-pressure synthetic techniques have been employed. $CaCu_3Ga_2Ru_2O_{12}$ [59] crystallises in space group *Im*$\bar{3}$, however the Ga^{3+} and Ru^{5+} cations re-

Composition	Pressure (GPa)	Temperature (°C)	Structure type	Space group	Ref.
$BiCoO_3$	6	970	Pv	*P*4*mm*	[70]
$Sr_{1-x}Ca_xCoO_3$	6	1200 – 1300	Pv, ss	*Pm*$\bar{3}$*m*	[71]
$Sr_{2-y}Y_yCoO_4$	6	1000 – 1350	RP1, ss	*I*4/*mmm*	[72]
$SrRhO_3$	6	1500	Pv	*Pnma*	[73]
$Sr_{1-x}Ca_xRhO_3$	6	1500	Pv, ss	*Pnma*	[74]
$Sr_3Rh_2O_7$	6	1500	RP2	*Ccca*	[75]
$Sr_4Rh_3O_{10}$	6	1500	RP3	*Pbam*	[76]

Table 7. Composition, reported synthesis pressures and temperatures, structure type, space group and references for materials containing cobalt group B-site cations.

main disordered over the perovskite B-sites. Transport measurements show it to be a Pauli paramagnetic conductor, and this behaviour is thought to originate from a $Cu^{2+} + Ru^{5+} \rightarrow Cu^{3+} + Ru^{4+}$ valence degeneracy. The solid solution $Sr_{3-x}Ba_xCaRu_2O_9$ has also been stabilised over the full substitution range $0 < x < 3$ [60], with the Ba end member adopting a 1 : 2 B-site cation ordered structure with no tilting of the (Ca/Ru) octahedra.

Cobalt group

$BiCoO_3$, considered a candidate material for multiferroic behaviour owing to its combination of the polarisable Bi^{3+} cation, and the magnetic high spin Co^{3+} ion, has recently been synthesised for the first time under high-pressure conditions [70]. The r. t. crystal structure is tetragonal, *P*4*mm*, with a very large *c/a* ratio = 1.27. Magnetic measurements and neutron diffraction studies evidence a magnetic transition at 470 K, and a C-type antiferromagnetic structure is proposed with the magnetic moments of Co^{3+} aligning antiferromagnetically in the *ab* plane, but stacking ferromagnetically along the *c* axis. Resistivity measurements suggest that $BiCoO_3$ is an insulator at all temperatures.

The solid solution series $Sr_{1-x}Ca_xCoO_3$ has been prepared under HPHT conditions [71] for $0 \leq x \leq 0.8$, and all the samples were found to be cubic perovskites. The end member, $SrCoO_3$, exhibits a ferromagnetic transition with a Curie temperature of $T_C \sim 266$ K, which increases slightly to 286 K at $x = 0.2$ before rapidly falling off at higher doping levels. Resistivity measurements evidence metallic behaviour at $x = 0.1$, and semiconducting behaviour for $0.2 \leq x \leq 0.4$, before almost reverting to metallic behaviour above $x = 0.6$. A negative magnetoresistance of $\sim 5.5\%$ was observed in the region of T_C for $x = 0$ and 0.2.

The K_2NiO_4-type (Fig. 1c) cobalt oxide, Sr_2CoO_4, containing only Co^{4+} ions has been synthesised by HPHT [72], and is shown to crystallise in space group *I*4/*mmm*. A ferromagnetic transition has been observed in this material with $T_C = 255$ K, while resistivity measurements evidence semiconductor behaviour and a negative magnetoresistance effect. Electron doping, by means of substitution of Y^{3+} for Sr^{2+}, suppresses the ferromagnetism, with T_C dropping to 150 K for $x = 0.5$, and then no ferromagnetism being observed above $x = 0.67$. Sample resistivity is also seen to increase with yttrium doping.

The rhodium(IV) oxide perovskite $SrRhO_3$ was recently obtained by high-pressure synthesis [73], and was found to adopt the distorted $GdFeO_3$-type *Pnma* structure. Resistivity measurements suggest Fermi liquid behaviour, with no long range magnetic order being observed above 1.8 K. Isovalent doping of Sr^{2+} by Ca^{2+} was also achieved [74], with no change in structure type and no remarkable change in the magnetic or electrical properties. The $n = 2$ (Fig. 1d) and $n = 3$ Ruddlesden-Popper phases $Sr_3Rh_2O_7$ and $Sr_4Rh_3O_{10}$ have also recently been prepared for the first time under analogous conditions [75, 76], but again no clear signs of magnetic or electrical transitions were observed above 2 K.

Nickel group

The nickelate perovskites *RE*NiO_3, first reported 35 years ago [81], require increasingly high pressures to stabilise Ni^{3+} for progressively smaller rare earths, RE^{3+}, in the perovskite structure. These materials show metal-to-insulator (MI) transitions as a function of temperature that vary systematically with the rare-earth size, *RE*. Research prior to 1996 is reviewed in [82], while more recent studies [83 – 90] have shown that a transition to a monoclinic charge disproportionated phase ($2Ni^{3+} \rightarrow Ni^{3+\delta} + Ni^{3-\delta}$) occurs below the MI transition. Two new nickelates have been reported using high-pressure synthesis techniques – $TlNiO_3$ [77, 91] and $BiNiO_3$ [78].

Powder X-ray refinements suggested that $TlNiO_3$ adopts an orthorhombic $GdFeO_3$-type structure, with no evidence of nickel charge disproportionation. The coordination polyhedron around the thallium cations

Composition	Pressure (GPa)	Temperature (°C)	Structure type	Space group	Ref.
$TlNiO_3$	7.5	650 – 700	Pv	$P2_1/n$	[77]
$BiNiO_3$	6	1000	Pv	$P\bar{1}$	[78]
$Bi_{1-x}La_xNiO_3$	6	1000	Pv, ss	$P\bar{1}$, *Pnma*	[79]
$LaPdO_3$	5	1100 – 1150	Pv	*Pnma*	[80]

Table 8. Composition, reported synthesis pressures and temperatures, structure type, space group and references for materials containing nickel group B-site cations.

Table 9. Composition, reported synthesis pressures and temperatures, structure type, space group and references for materials containing copper group B-site cations.

Composition	Pressure (GPa)	Temperature (°C)	Structure type	Space group	Ref.
$NdCuO_{3-\delta}$	10	1000	Pv	*Pbam*, *P*2/*m*, *Pbnm*	[92]
Ln_2CuMO_6 (Ln = La, Pr, Nd, Sm; M = Sn, Zr)	6 – 8	1000 – 1200	Pv, B	$P2_1/m$	[93]
Ba_2CuTeO_6	5	900	Pv, B	*I*4/*m*	[94]
$SeCu_{1-x}Zn_xO_3$	6	900 – 1000	Pv, ss	*Pnma*	[95]

is, however, somewhat unusual with the twelve Tl–O bonds appearing to fall into three distinct groups (four short, four medium, and four long distances) – an effect attributed to the relatively covalent nature of the Tl–O bonds, in comparison with those of the rare earth elements. This covalency effect is also thought to be responsible for the lower than expected Néel temperature in $TlNiO_3$ (T_N = 105 K, although the Ni–O–Ni superexchange angle is similar to that observed in $YNiO_3$ with T_N = 145 K), as the strongly covalent Tl–O bonds weaken the Ni–O bonds, leading to a relatively weak orbital overlap. A subsequent neutron diffraction study [77] however yielded better structural refinements in the monoclinic space group $P2_1/n$, with two crystallographic Ni sites. Mössbauer measurements on a ^{57}Fe-doped sample confirmed the existence of two octahedral sites in $TlNiO_3$, and this is consistent with the Ni^{3+} disproportionation observed in other $RNiO_3$ perovskites.

$BiNiO_3$ by contrast was shown to have a heavily distorted triclinic unit cell, space group $P\bar{1}$. Precise structural analysis from a synchrotron XRD study revealed that the Bi atoms were disproportionated to Bi^{3+} and Bi^{5+}, and therefore that the oxidation states were $Bi^{3+}{}_{1/2}Bi^{5+}{}_{1/2}Ni^{2+}O_3$ rather than $Bi^{3+}Ni^{3+}O_3$. Electrical resistivity measurements showed $BiNiO_3$ to be insulating, consistent with the presence of Ni^{2+}, whilst magnetic measurements suggested weak ferromagnetic behaviour. Further study [79] showed that a melting of this A-site charge disproportionation, yielding a metallic, orthorhombic *Pnma* phase, could be achieved either by replacement of Bi with 7.5% La^{3+}, or by application of high pressures (3 GPa) or high temperatures (near 340 K for x = 0.05).

$LaPdO_3$ has been prepared by HPHT synthesis [80]. EXAFS and XANES studies show that $LaPdO_3$ is the first perovskite oxide to stabilise trivalent palladium, despite the tendency of the Pd^{3+} ion to disproportionate into Pd^{2+} and Pd^4.

Copper group

Layered high-temperature superconducting cuprates are a large class of materials including many HPHT phases that are not reviewed here; several review papers can be found elsewhere [7, 96 – 100]. A related series of five new oxygen-deficient $NdCuO_{3-\delta}$ perovskites has been prepared by high-pressure synthesis [92]. Each displays a distinct oxygen vacancy ordering, dependent on both δ and the synthetic conditions. For example $NdCuO_{2.5}$ crystallises in an orthorhombic $\sqrt{2}a_p \times 2\sqrt{2}a_p \times a_p$ subcell, consisting entirely of corner-sharing CuO_5 square pyramids. While the phases are metallic for $\delta < 0.5$, superconductivity was not observed in this system down to 4.2 K.

A series of Cu-containing double perovskites have been prepared by high-pressure synthesis – RE_2CuSnO_6 (*RE* = Pr, Nd, Sm) [93], La_2CuZrO_6 [93] and Ba_2CuTeO_6 [94]. Ba_2CuTeO_6 crystallises in tetragonal space group *I*4/*m*, with the Cu^{2+} and Te^{6+} ions fully ordered in a rocksalt arrangement. Magnetisation measurements evidence two-dimensional antiferromagnetism below 100 K, due to superexchange interactions between Cu^{2+} ions in the *ab* plane, mediated by the nonmagnetic ions. The other double perovskites, however, adopt a layered configuration of B cations, as previously observed for La_2CuSnO_6 [101]. Replacement of La by smaller lanthanides, or indeed replacement of Sn^{4+} by the larger Zr^{4+}, leads to an increased buckling in the Cu–O–Cu bonds in the CuO_2 layers of this structure, with a resulting decrease of the antiferromagnetic ordering temperature of this system.

$SeCuO_3$ [102, 103] and the $SeMO_3$ analogues (M = Mn, Co, Ni) [102, 104, 105] represent a class of

perovskites that can only be made at high pressure. The small size of the Se^{4+} cation, coupled with high polarisability due to the non-bonded s-electron pair, leads to very distorted perovskite structures. $SeCuO_3$ is ferromagnetic below T_C = 25 K, and a large magnetocapacitance has been measured close to the transition temperature [102]. New solid solutions $SeCu_{1-x}Zn_xO_3$ have been prepared under HPHT conditions [95]. They have a distorted orthorombic $GdFeO_3$-type structure, space group *Pnma*, at all doping levels. The Weiss constant and T_C both decrease progressively as Cu^{2+} is replaced by non-magnetic Zn^{2+}.

Discussion

The above results demonstrate that HPHT synthesis remains an important and popular method for discovery of transition metal oxide perovskites, with over 60 new materials reported during the last decade. Both cation ordered and disordered perovskites have been prepared. Continuous solid solutions were found *e. g.* for the $BiScO_3$ – $PbTiO_3$ system, but cation ordering on the A (*e. g.* $CaFeTi_2O_6$) or B (*e. g.* Bi_2MnNiO_6) or both (*e. g.* $CaCu_3Cr_2Sb_2O_{12}$) sites is observed in many systems. The prevalence of partial or complete A site ordering (even of cations having the same charge, such as Ca^{2+} and Fe^{2+} in the former example) is particularly notable as it is rare in perovskites prepared at ambient pressure. This reflects the accentuation of A cation size differences at high pressures. Ca^{2+}/Cu^{2+} order is assisted by crystal field effects that stabilise Cu^{2+} in a square planar environment.

In contrast to the preparation of mixed cation materials, HPHT syntheses of oxygen-deficient perovskites are rare, perhaps because of the difficulty in controlling oxygen fugacities at high pressure. However, the series of new oxygen-vacancy ordered $NdCuO_{3-\delta}$ phases characterised by electron microscopy shows that there is considerable scope for other oxygen-deficient structures to be prepared.

The syntheses of many perovskite phases have been driven by the search for specific materials properties. Sc^{3+} and Ti^{4+} perovskites are of continuing importance for ferroelectric properties. In addition, the search for multiferroic materials, having both ferroelectric and ferromagnetic order, has led to the (re)investigation of many Bi^{3+} and Se^{4+} perovskites. Significant magnetocapacitances have been found at low temperatures in $BiMnO_3$ and $SeCuO_3$. Bi_2MnNiO_6 is notable as a successful design of a multiferroic prepared at HPHT.

Mixed or unusual oxidation states can give rise to interesting electronic properties such as metal-insulator transitions. $LaPdO_3$ provides the first example of a perovskite containing Pd^{3+}, while charge transfer between Cr and Ru leads to two composition-driven metal-insulator transitions in the $SrCr_xRu_{1-x}O_3$ system, and an unusual charge ordering of Bi^{3+} and Bi^{5+} states over perovskite A sites is observed in $BiNiO_3$. Investigation of CMR and associated properties in manganese oxide perovskites has led to the synthesis of several high-pressure analogues. CMR and high Curie temperatures were discovered in the new high-pressure $LnCu_3Mn_4O_{12}$ phases, while $NaMn_3Mn_4O_{12}$ shows a robust Mn^{3+}/Mn^{4+} charge ordering. High pressure continues to yield new superconducting layered cuprates (reviewed elsewhere), and both rocksalt and layered cation orderings are found within double perovskites of Cu^{2+}.

In conclusion, it is evident that HPHT synthesis remains an important source of new transition metal oxide perovskites. Important developments from the last decade have included complex cation orderings on A and B sites, multiferroic Bi perovskites, and new manganites showing CMR and charge ordering properties.

Acknowledgements

We thank the EPSRC and the Leverhulme Trust for support.

[1] R. H. Mitchell, Perovskites: Modern and Ancient, Almaz Press Inc., Ontario 2002.
[2] J. B. Goodenough, Rep. Prog. Phys. **67**, 1915 (2004).
[3] A. S. Bhalla, R. Y. Guo, R. Roy, Mater. Res. Innov. **4**, 3 (2000).
[4] V. Thangadurai, W. Weppner, Ionics **12**, 81 (2006).
[5] M. A. Keane, J. Mater. Sci. **38**, 4661 (2003).
[6] G. Van Tendeloo, O. I. Lebedev, M. Hervieu, B. Raveau, Rep. Prog. Phys. **67**, 1315 (2004).
[7] M. Karppinen, H. Yamauchi, Mater. Sci. & Eng. R-Reports **26**, 51 (1999).
[8] P. M. Woodward, Acta Crystallogr. **B53**, 32 (1997).
[9] A. M. Glazer, Acta Crystallogr. **B28**, 3384 (1972).
[10] A. A. Belik, S. Iikubo, K. Kodama, N. Igawa, S. Shamoto, M. Maie, T. Nagai, Y. Matsui, S. Y. Stefanovich, B. I. Lazoryak, E. Takayama-Muromachi, J. Am. Chem. Soc. **128**, 706 (2006).
[11] Y. Inaguma, A. Miyaguchi, M. Yoshida, T. Katsumata,

Y. Shimojo, R. P. Wang, T. Sekiya, J. Appl. Phys. **95**, 231 (2004).
[12] C. Michel, J. M. Moreau, G. D. Achenbach, R. Gerson, W. J. James, Solid State Commun. **7**, 701 (1969).
[13] F. Kubel, H. Schmid, Acta Crystallogr. **B46**, 698 (1990).
[14] J. Wang, J. B. Neaton, H. Zheng, V. Nagarajan, S. B. Ogale, B. Liu, D. Viehland, V. Vaithyanathan, D. G. Schlom, U. V. Waghmare, N. A. Spaldin, K. M. Rabe, M. Wuttig, R. Ramesh, Science **299**, 1719 (2003).
[15] F. Sugawara, S. Iiida, Y. Syono, S. I. Akimoto, J. Phys. Soc. Jpn. **25**, 1553 (1968).
[16] T. Atou, H. Chiba, K. Ohoyama, Y. Yamaguchi, Y. Syono, J. Solid State Chem. **145**, 639 (1999).
[17] R. Seshadri, N. A. Hill, Chem. Mater. **13**, 2892 (2001).
[18] A. M. dos Santos, S. Parashar, A. R. Raju, Y. S. Zhao, A. K. Cheetham, C. N. R. Rao, Solid State Commun. **122**, 49 (2002).
[19] A. M. dos Santos, A. K. Cheetham, T. Atou, Y. Syono, Y. Yamaguchi, K. Ohoyama, H. Chiba, C. N. R. Rao, Phys. Rev. B **66**, (2002).
[20] T. Kimura, S. Kawamoto, I. Yamada, M. Azuma, M. Takano, Y. Tokura, Phys. Rev. B **67**, 180401 (2003).
[21] J. P. Miao, Z. Lu, L. P. Li, F. L. Ning, Z. G. Liu, X. Q. Huang, Y. Sui, Z. N. Qian, W. H. Su, J. Alloys Compd. **387**, 287 (2005).
[22] J. P. Miao, Z. Lu, Y. Sui, X. Q. Huang, Z. G. Liu, Z. N. Qian, Z. R. Zheng, Z. G. Zhang, W. H. Su, J. Alloys Compd. **399**, 256 (2005).
[23] A. R. Chakhmouradian, R. H. Mitchell, Am. Mineral **86**, 1076 (2001).
[24] J. H. Park, P. M. Woodward, J. B. Parise, Chem. Mater. **10**, 3092 (1998).
[25] K. Leinenweber, J. Parise, Am. Mineral **82**, 475 (1997).
[26] K. Leinenweber, J. Parise, J. Solid State Chem. **114**, 277 (1995).
[27] J. H. Park, P. M. Woodward, J. B. Parise, R. J. Reeder, I. Lubomirsky, O. Stafsudd, Chem. Mater. **11**, 177 (1999).
[28] A. J. Williams, J. P. Attfield, Phys. Rev. B **72**, 024436 (2005).
[29] P. Karen, P. M. Woodward, J. Linden, T. Vogt, A. Studer, P. Fischer, Phys. Rev. B **6421**, 214405 (2001).
[30] T. Vogt, P. M. Woodward, P. Karen, B. A. Hunter, P. Henning, A. R. Moodenbaugh, Phys. Rev. Lett. **84**, 2969 (2000).
[31] R. V. Shpanchenko, V. V. Chernaya, A. A. Tsirlin, P. S. Chizhov, D. E. Sklovsky, E. V. Antipov, E. P. Khlybov, V. Pomjakushin, A. M. Balagurov, J. E. Medvedeva, E. E. Kaul, C. Geibel, Chem. Mater. **16**, 3267 (2004).
[32] A. A. Belik, E. Takayama-Muromachi, J. Solid State Chem. **179**, 1650 (2006).
[33] A. N. Salak, N. P. Vyshatko, V. M. Ferreira, N. M. Olekhnovich, A. D. Shilin, Mater. Res. Bull. **38**, 453 (2003).
[34] S. H. Byeon, H. Kim, J. J. Yoon, Y. Dong, H. Yun, Y. Inaguma, M. Itoh, Chem. Mater. **10**, 2317 (1998).
[35] S. H. Byeon, M. W. Lufaso, J. B. Parise, P. M. Woodward, T. Hansen, Chem. Mater. **15**, 3798 (2003).
[36] B. L. Chamberland, P. S. Danielson, J. Solid State Chem. **3**, 243 (1971).
[37] G. Liu, J. E. Greedan, J. Solid State Chem. **110**, 274 (1994).
[38] J. Garciajaca, J. I. R. Larramendi, M. Insausti, M. I. Arriortua, T. Rojo, J. Mater. Chem. **5**, 1995 (1995).
[39] G. A. Smolenskii, A. I. Agranovskaia, S. N. Popov, V. A. Isupov, Sov. Phys. – Tech. Phys. **3**, 1981 (1958).
[40] N. Lampis, P. Sciau, A. G. Lehmann, J. Phys.: Condens. Matter **11**, 3489 (1999).
[41] S. A. Ivanov, R. Tellgren, H. Rundlof, N. W. Thomas, S. Ananta, J. Phys.: Condens. Matter **12**, 2393 (2000).
[42] S. Niitaka, M. Azuma, M. Takano, E. Nishibori, M. Takata, M. Sakata, Solid State Ionics **172**, 557 (2004).
[43] A. J. Williams, A. Gillies, J. P. Attfield, G. Heymann, H. Huppertz, M. J. Martinez-Lope, J. A. Alonso, Phys. Rev. B **73**, 104409 (2006).
[44] S. H. Byeon, S. S. Lee, J. B. Parise, P. M. Woodward, N. H. Hur, Chem. Mater. **17**, 3552 (2005).
[45] D. A. Vander Griend, S. Boudin, K. R. Poeppelmeier, M. Azuma, H. Toganoh, M. Takano, J. Am. Chem. Soc. **120**, 11518 (1998).
[46] D. A. Vander Griend, K. R. Poeppelmeier, H. Toganoh, M. Azuma, M. Takano, Physica C **341**, 335 (2000).
[47] I. O. Troyanchuk, D. D. Khalyavin, H. Szymczak, Mater. Res. Bull. **32**, 1637 (1997).
[48] J. Sanchez-Benitez, J. A. Alonso, H. Falcon, M. J. Martinez-Lope, A. De Andres, M. T. Fernandez-Diaz, J. Phys.: Condens. Matter **17**, S3063 (2005).
[49] J. A. Alonso, J. Sanchez-Benitez, A. De Andres, M. J. Martinez-Lope, M. T. Casais, J. L. Martinez, Appl. Phys. Lett. **83**, 2623 (2003).
[50] A. Prodi, E. Gilioli, A. Gauzzi, F. Licci, M. Marezio, F. Bolzoni, Q. Huang, A. Santoro, J. W. Lynn, Nature Mater. **3**, 48 (2004).
[51] M. Azuma, K. Takata, T. Saito, S. Ishiwata, Y. Shimakawa, M. Takano, J. Am. Chem. Soc. **127**, 8889 (2005).
[52] E. Takayama-Muromachi, T. Drezen, M. Isobe, N. D. Zhigadlo, K. Kimoto, Y. Matsui, E. Kita, J. Solid State Chem. **175**, 366 (2003).
[53] A. Waintal, J. Chenavas, Mater. Res. Bull. **2**, 819 (1967).
[54] M. Marezio, P. D. Dernier, J. Chenavas, J. C. Joubert, J. Solid State Chem. **6**, 16 (1973).
[55] T. Takeda, R. Kanno, Y. Kawamoto, M. Takano,

S. Kawasaki, T. Kamiyama, F. Izumi, Solid State Sci. **2**, 673 (2000).
[56] S. Kawasaki, M. Takano, Y. Takeda, Solid State Ionics **108**, 221 (1998).
[57] I. O. Troyanchuk, L. S. Lobanovsky, H. Szymczak, K. Barner, J. Magn. Magn. Mater. **219**, 163 (2000).
[58] K. Yamaura, D. P. Young, E. Takayama-Muromachi, Phys. Rev. B **69**, 024410 (2004).
[59] S. H. Byeon, S. S. Lee, J. B. Parise, P. M. Woodward, N. H. Hur, Chem. Mater. **16**, 3697 (2004).
[60] J. T. Rijssenbeek, T. Saito, S. Malo, A. T. Masaki, M. Takano, K. R. Poeppelmeier, J. Am. Chem. Soc. **127**, 675 (2005).
[61] P. M. Woodward, D. E. Cox, E. Moshopoulou, A. W. Sleight, S. Morimoto, Phys. Rev. B **62**, 844 (2000).
[62] Y. Maeno, H. Hashimoto, K. Yoshida, S. Nishizaki, T. Fujita, J. G. Bednorz, F. Lichtenberg, Nature **372**, 532 (1994).
[63] L. Klein, J. S. Dodge, C. H. Ahn, G. J. Snyder, T. H. Geballe, M. R. Beasley, A. Kapitulnik, Phys. Rev. Lett. **77**, 2774 (1996).
[64] K. P. Hong, Y. H. Choi, Y. U. Kwon, D. Y. Jung, J. S. Lee, H. S. Shim, C. H. Lee, J. Solid State Chem. **150**, 383 (2000).
[65] Y. Izumiyama, Y. Doi, M. Wakeshima, Y. Hinatsu, K. Oikawa, Y. Shimojo, Y. Morii, J. Mater. Chem. **10**, 2364 (2000).
[66] Y. Izumiyama, Y. Doi, M. Wakeshima, Y. Hinatsu, Y. Shimojo, Y. Morii, J. Phys.: Condens. Matter **13**, 1303 (2001).
[67] Y. Izumiyama, Y. Doi, M. Wakeshima, Y. Hinatsu, A. Nakamura, Y. Ishii, J. Solid State Chem. **169**, 125 (2002).
[68] P. D. Battle, C. P. Grey, M. Hervieu, C. Martin, C. A. Moore, Y. Paik, J. Solid State Chem. **175**, 20 (2003).
[69] Y. Doi, Y. Hinatsu, A. Nakamura, Y. Ishii, Y. Morii, J. Mater. Chem. **13**, 1758 (2003).
[70] A. A. Belik, S. Iikubo, K. Kodama, N. Igawa, S. Shamoto, S. Niitaka, M. Azuma, Y. Shimakawa, M. Takano, F. Izumi, E. Takayama-Muromaychi, Chem. Mater. **18**, 798 (2006).
[71] S. Balamurugan, M. Xu, E. Takayama-Muromachi, J. Solid State Chem. **178**, 3431 (2005).
[72] X. L. Wang, E. Takayama-Muromachi, Phys. Rev. B **72**, 064401 (2005).
[73] K. Yamaura, E. Takayama-Muromachi, Phys. Rev. B **64**, 224424 (2001).
[74] K. Yamaura, Q. Huang, D. P. Young, M. Arai, E. Takayama-Muromachi, Physica B **329**, 820 (2003).
[75] K. Yamaura, Q. Huang, D. P. Young, Y. Noguchi, E. Takayama-Muromachi, Phys. Rev. B **66**, 134431 (2002).
[76] K. Yamaura, Q. Z. Huang, D. P. Young, E. Takayama-Muromachi, Chem. Mater. **16**, 3424 (2004).
[77] S. J. Kim, M. J. Martinez-Lope, M. T. Fernandez-Diaz, J. A. Alonso, I. Presniakov, G. Demazeau, Chem. Mater. **14**, 4926 (2002).
[78] S. Ishiwata, M. Azuma, M. Takano, E. Nishibori, M. Takata, M. Sakata, K. Kato, J. Mater. Chem. **12**, 3733 (2002).
[79] S. Ishiwata, M. Azuma, M. Hanawa, Y. Moritomo, Y. Ohishi, K. Kato, M. Takata, E. Nishibori, M. Sakata, I. Terasaki, M. Takano, Phys. Rev. B **72**, 045104 (2005).
[80] S. J. Kim, S. Lemaux, G. Demazeau, J. Y. Kim, J. H. Choy, J. Am. Chem. Soc. **123**, 10413 (2001).
[81] G. Demazeau, A. Marbeuf, M. Pouchard, W. Hagenmul, J. B. Goodenough, C. R. Seances Acad. Sci., Ser. B **272**, 2163 (1971).
[82] M. L. Medarde, J. Phys.: Condens. Matter **9**, 1679 (1997).
[83] J. A. Alonso, J. L. Garcia-Munoz, M. T. Fernandez-Diaz, M. A. G. Aranda, M. J. Martinez-Lope, M. T. Casais, Phys. Rev. Lett. **82**, 3871 (1999).
[84] J. A. Alonso, M. J. Martinez-Lope, M. T. Casais, M. A. G. Aranda, M. T. Fernandez-Diaz, J. Am. Chem. Soc. **121**, 4754 (1999).
[85] J. A. Alonso, M. J. Martinez-Lope, M. T. Casais, J. L. Martinez, G. Demazeau, A. Largeteau, J. L. Garcia-Munoz, A. Munoz, M. T. Fernandez-Diaz, Chem. Mater. **11**, 2463 (1999).
[86] J. A. Alonso, M. J. Martinez-Lope, M. T. Casais, J. L. Garcia-Munoz, M. T. Fernandez-Diaz, Phys. Rev. B **61**, 1756 (2000).
[87] J. A. Alonso, M. J. Martinez-Lope, M. T. Casais, J. L. Garcia-Munoz, M. T. Fernandez-Diaz, M. A. Aranda, Phys. Rev. B **64**, 094102 (2001).
[88] T. Saito, M. Azuma, E. Nishibori, M. Takata, M. Sakata, N. Nakayama, T. Arima, T. Kimura, C. Urano, M. Takano, Physica B **329**, 866 (2003).
[89] J. S. Zhou, J. B. Goodenough, Phys. Rev. B **69**, 153105 (2004).
[90] M. Amboage, M. Hanfland, J. A. Alonso, M. J. Martinez-Lope, J. Phys.: Condens. Matter **17**, S783 (2005).
[91] S. J. Kim, G. Demazeau, J. A. Alonso, J. H. Choy, J. Mater. Chem. **11**, 487 (2001).
[92] B. H. Chen, D. Walker, E. Suard, B. A. Scott, B. Mercey, M. Hervieu, B. Raveau, Inorg. Chem. **34**, 2077 (1995).
[93] M. Azuma, S. Kaimori, M. Takano, Chem. Mater. **10**, 3124 (1998).
[94] D. Iwanaga, Y. Inaguma, M. Itoh, J. Solid State Chem. **147**, 291 (1999).
[95] R. Escamilla, J. M. Gallardo-Amores, E. Moran, M. A. Alario-Franco, J. Solid State Chem. **168**, 149 (2002).
[96] E. Takayama-Muromachi, Chem. Mater. **10**, 2686 (1998).

[97] M. T. Weller, C. S. Knee, J. Mater. Chem. **11**, 701 (2001).
[98] Y. H. Liu, G. C. Che, K. Q. Li, Z. X. Zhao, Physica C **422**, 88 (2005).
[99] R. Ruiz-Bustos, M. H. Aguirre, M. A. Alario-Franco, Inorg. Chem. **44**, 3063 (2005).
[100] A. Dos Santos-Garcia, M. H. Aguirre, E. Moran, R. S. Puche, M. A. Alario-Franco, J. Solid State Chem. **179**, 1296 (2006).
[101] M. T. Anderson, K. R. Poeppelmeier, Chem. Mater. **3**, 476 (1991).
[102] K. Kohn, K. Inoue, O. Horie, S. Akimoto, J. Solid State Chem. **18**, 27 (1976).
[103] G. Lawes, A. P. Ramirez, C. M. Varma, M. A. Subramanian, Phys. Rev. Lett. **91**, 257208 (2003).
[104] R. Escamilla, A. Duran, M. I. Rosales, E. Moran, M. A. Alario-Franco, J. Phys.: Condens. Matter **15**, 1951 (2003).
[105] A. Munoz, J. A. Alonso, M. J. Martinez-Lope, E. Moran, R. Escamilla, Phys. Rev. B **73**, 104442 (2006).